

TOHAN: A One-step Approach towards Few-shot Hypothesis Adaptation

Haoang Chi^{*1}, Feng Liu^{*2}, Wenjing Yang¹, Long Lan¹, Tongliang Liu³,
Bo Han⁴, William K. Cheung⁴, and James T. Kwok⁵

¹Institute for Quantum Information & State Key Laboratory of High Performance Computing, National University of Defense Technology

²DeSI Lab, AAII, University of Technology Sydney

³TML Lab, University of Sydney

⁴Department of Computer Science, Hong Kong Baptist University

⁵Department of Computer Science and Engineering, Hong Kong University of Science and Technology

Abstract

In *few-shot domain adaptation* (FDA), classifiers for the target domain are trained with *accessible* labeled data in the *source domain* (SD) and few labeled data in the *target domain* (TD). However, data usually contain private information in the current era, e.g., data distributed on personal phones. Thus, the private information will be leaked if we directly access data in SD to train a target-domain classifier (required by FDA methods). In this paper, to thoroughly prevent the privacy leakage in SD, we consider a very challenging problem setting, where the classifier for the TD has to be trained using few labeled target data and a well-trained SD classifier, named *few-shot hypothesis adaptation* (FHA). In FHA, we cannot access data in SD, as a result, the private information in SD will be protected well. To this end, we propose a *target orientated hypothesis adaptation network* (TOHAN) to solve the FHA problem, where we generate highly-compatible unlabeled data (i.e., an intermediate domain) to help train a target-domain classifier. TOHAN maintains two deep networks simultaneously, where one focuses on learning an intermediate domain and the other takes care of the intermediate-to-target distributional adaptation and the target-risk minimization. Experimental results show that TOHAN outperforms competitive baselines significantly.

1 Introduction

In *Domain Adaptation* (DA) [6, 16, 36, 37, 45, 52], we aim to train a target-domain classifier with data in source and target domains. Based on the availability of data in the target domain (e.g., fully-labeled data, partially-labeled data and unlabeled data), DA is divided into three categories: *supervised DA* (SDA) [38], semi-supervised DA [15] and *unsupervised DA* (UDA) [7, 23, 34, 55]. Since SDA methods outperform UDA methods for the same quantity of target data [28], it becomes attractive if we can train a good target-domain classifier using labeled-source data and few labeled-target data [40].

Hence, *few-shot domain adaptation* (FDA) methods [28] are proposed to train a target-domain classifier with *accessible* labeled data from the source domain and few labeled data from the target domain.

^{*}Equal contributions.

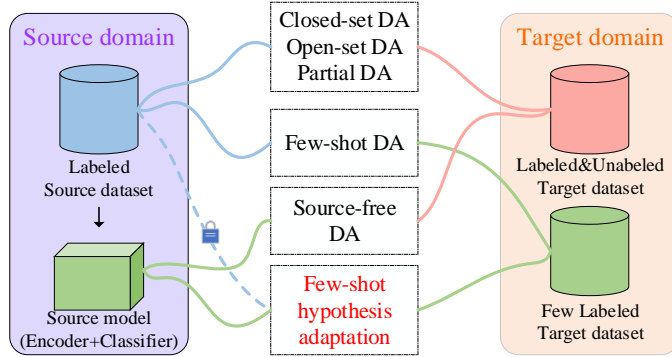


Figure 1: The *few-shot hypothesis adaptation* (FHA) and existing domain adaptation problem settings. In FHA, we aim to train a classifier for the target domain only using few labeled target data and a well-trained source-domain classifier. Namely, we do not access any source data when training the target-domain classifier. This thoroughly prevents the information leakage of the source domain. The lock means we cannot access data in the source domain.

Compared to SDA and UDA methods, FDA methods only require few data in the target domain, which is suitable to solve many problems, e.g., medical image processing [42]. Existing FDA methods involve many approaches and applications. Structural causal model [40] has been proposed to overcome the problem caused by apparent distribution discrepancy. Since deep neural networks tend to overfit the few-labeled data in the training process, a meta-learning method becomes an effective solution to the FDA problem [39]. Besides, FDA methods perform well in face of generation [46] and virtual-to-real scene parsing [50].

However, it is risky to directly access source data for training a target-domain classifier (required by FDA methods) due to the private information contained in the source domain. In the current era, labeled data are distributed over different physical devices and usually contain private information, e.g., data on personal phones or from surveillance cameras [21]. Since FDA methods [40] require abundant labeled source data to train a target-domain classifier, they may leak private information in the training process, maybe resulting in massive loss [14].

In this paper, to thoroughly prevent the private-information leakage of the source domain in existing FDA methods, we propose a novel and very challenging setting, where the classifier for the target domain has to be trained using few labeled target data and a well-trained source-domain classifier, named *few-shot hypothesis adaptation* (FHA, see Figure 1). In the literature, researchers have adapted source-domain hypothesis to be a target-domain classifier when abundant unlabeled target data are available [21]. However, since these methods require abundant target data, they cannot address the FHA problem well, which has been empirically verified in Table 1 and Table 2.

The key benefit of FHA is that we do not need to access any source data, which wisely avoids the private-information leakage of the source domain. Moreover, the scales of images of most domains tend to be larger in the real world. Thus, existing FDA methods will take a long time to train a target-domain classifier. However, in FHA, we can train a target-domain classifier only using a well-trained source-domain classifier and few labeled target data.

To address FHA, we first revisit the theory related to learning from few labeled data and try to find out if FHA can be addressed in principle. Fortunately, we find that, in *semi-supervised learning* (SSL) where only few labeled data available, researchers have already shown that, a good classifier can be learned if we have abundant unlabeled data that are compatible with the labeled data. Thus, motivated by the SSL, we aim to address FHA via gradually generating highly compatible data for the target domain. To this

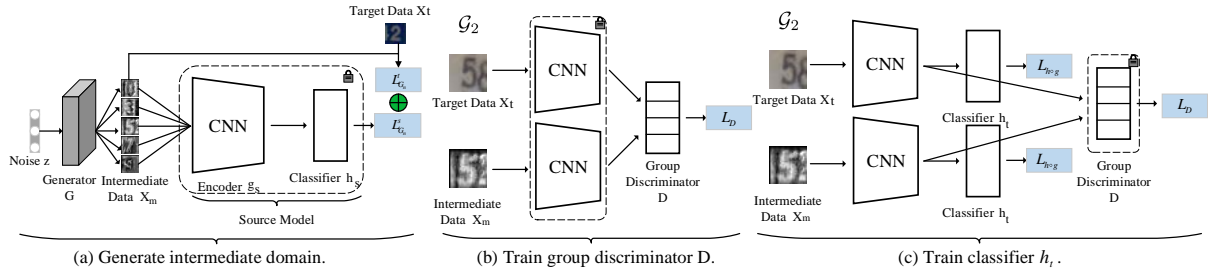


Figure 2: Overview of *target orientated hypothesis adaptation network* (TOHAN). It consists of generator G , encoder g_s , g_t (initialize $g_t=g_s$), classifier h_s , h_t (initialize $h_t=h_s$) and group discriminator D . (a) Firstly, we train a generator G using the source classifier g_s , h_s and target data D_t , then we generate intermediate data between two domains. (b) We freeze g_t and h_t and update group discriminator D . (c) We freeze D and update g_t and h_t . In subfigures (b) and (c), they show a data pair from \mathcal{G}_2 which two data come from the same class but different domain.

end, we propose a *target orientated hypothesis adaptation network* (TOHAN) to solve the FHA problem. TOHAN maintains two deep networks simultaneously, where one focuses on learning an intermediate domain (i.e., learning compatible data) and the other takes care of the intermediate-to-target distributional adaptation (Figure 2).

Specifically, due to the scarcity of target data, we cannot directly generate compatible data for the target domain. Thus, we first generate an intermediate domain where data are compatible with the given source classifier and the few labeled target data. Then, we conduct the intermediate-to-target distributional adaptation to make the generated intermediate domain close to the target domain. Eventually, we embed the above procedures into our one-step solution, TOHAN, to make us be able to gradually generate an intermediate domain that contains highly compatible data for the target domain. According to learnability of SSL, with the generated “target-like” intermediate domain, TOHAN can learn a good target-domain classifier.

We conduct experiments on 8 FHA tasks on 5 datasets (*MNIST*, *SVHN*, *USPS*, *CIFAR-10* and *STL-10*). We compare TOHAN with 5 competitive baselines. Experiments show that TOHAN effectively transfers knowledge of the source hypothesis to train a target-domain classifier when we only have few labeled target data. In a word, our paper opens a new door to domain adaptation field, which solves privacy leakage and data shortage simultaneously.

2 Few-shot Hypothesis Adaptation

In this section, we formalize a novel and challenging problem setting, called *few-shot hypothesis adaptation* (FHA). Let $\mathcal{X} \subset \mathbb{R}^d$ be a feature (input) space and $\mathcal{Y} := \{1, \dots, N\}$ be a label (output) space, and N is the number of classes. A domain for the FHA problem is defined as follows.

Definition 1 (Domains for FHA). *Given random variables $X_s, X_t \in \mathcal{X}$, $Y_s, Y_t \in \mathcal{Y}$, the source and target domains are joint distributions $P(X_s, Y_s)$ and $P(X_t, Y_t)$, where the joint distributions $P(X_s, Y_s) \neq P(X_t, Y_t)$ and \mathcal{X} is compact.*

Then the FHA problem is defined as follows.

Problem 1 (FHA). *Given a model (consisting of an encoder g_s and a classifier h_s) trained on the source domain $P(X_s, Y_s)$ and independent and identically distributed (i.i.d.) labeled data $D_t = \{(x_t^i, y_t^i)\}_{i=1}^{n_t}$*

($n_t \leq 7$, following [32]) drawn from the target domain $P(X_t, Y_t)$, the aim of FHA is to train a classifier $h_t : \mathcal{X} \rightarrow \mathcal{Y}$ with g_s , h_s and D_t such that h_t can accurately classify target data drawn from $P(X_t, Y_t)$.

Comparison with Few-shot Learning. The main difference between FHA and FSL is the prior knowledge [24, 25, 44, 47]. The prior knowledge of FSL mainly includes various types of numerical information and comes from the same distribution with their tasks [44]. For example, [43] uses the data itself as prior knowledge, and [35] uses the pairwise similarity, which is relatively weaker than the former. In addition, *model-agnostic meta learning* (MAML) requires data to optimize a meta-learner as prior knowledge [8]. However, the prior knowledge of FHA is just a well-trained classifier and training data of this classifier come from different distribution with $P(X_t, Y_t)$.

Comparison with UDA. The main differences between FHA and UDA [31, 48, 51, 53] focus on amount and label of data on two domains. For source domain, UDA requires a large amount of labeled data, while FHA only requires a well-trained model. For target domain, UDA requires a large amount of unlabeled data, while FHA requires *few* labeled data.

Comparison with Few-shot Domain Adaptation. With the development of FSL, researchers also apply ideas of FSL into domain adaptation, called *few-shot domain adaptation* (FDA). FADA [28] is a representative FDA method, which pairs data from source domain and data from target domain and then follows the adversarial domain adaptation method. Casual mechanism transfer [40] is another novel FDA method dealing with a meta-distributional scenario, in which the data generating mechanism is invariant among domains. Nevertheless, FDA methods still need to access many labeled source data for training, which may cause the private-information leakage of the source domain.

Comparison with Hypothesis Transfer Learning. In the *hypothesis transfer learning* (HTL), we can only access a well-trained source-domain classifier and small labeled or abundant unlabeled target data. [19] requires small labeled target data and uses the Leave-One-Out error find the optimal transfer parameters. Later, SHOT [21] is proposed to solve the HTL with many unlabeled target data by freezing the source-domain classifier and learning a target-specific feature extraction module. As for the universal setting, a two-stage learning process [18] has been proposed to address the HTL problem. Compared with FHA, HTL still requires at least small target data (e.g., at least 12 samples in binary classification problem [19], or at least two of labeling percentage [1]). In FHA, we focus on a more challenging situation: only few data (e.g., one sample per class) are available. Besides, previous solutions to HTL mainly focus on mortifying existing hypotheses or loss functions used for fine-tuning. However, our solution stems from the learnability of semi-supervised learning (Section 3) and try to generate more compatible data, which is quite different from previous works. In this paper, we modify the newest HTL method, SHOT [21], as one of our baselines. The modified SHOT can leverage labeled target data to train a good target-domain classifier.

3 How to Learn from Few-shot Data in Principle

From the view of statistical learning theory [41], it is unrealistic to directly learn an accurate target-domain classifier only with few labeled data. However, the amount of labeled data in *semi-supervised learning* (SSL) [56] is also few (e.g., one sample per class), but SSL methods still achieves good performance across various learning tasks, which motivates us to consider solving FHA in the view of SSL. First, we will show theoretical analysis regarding learnability of SSL.

Learnability of SSL. For simplicity, we consider the 0-1 semi-supervised classification problem. Let $c^* : \mathcal{X} \rightarrow \{0, 1\}$ be the optimal target classifier and $\mathcal{H} = \{h : \mathcal{X} \rightarrow \{0, 1\}\}$ is a hypothesis space. Let $err(h) = \mathbb{E}_{x \sim P}[h(x) \neq c^*(x)]$ be the true error rate of a hypothesis h over a distribution P . In SSL, its learnability mainly depends on the compatibility $\chi : \mathcal{H} \times \mathcal{X} \mapsto [0, 1]$ that measures how “compatible” h is to an unlabeled data x . Let $\chi(h, P) = \mathbb{E}_{x \sim P}[\chi(h, x)]$ be the expectation of compatibility of data from

P on a classifier h . If the unlabeled data and c^* are highly compatible (i.e., $\chi(c^*, P)$ closes to 1), then, in theory, we can learn a good classifier with few labeled data and sufficient unlabeled data. Specifically, we have the following theorem (see proof in Appendix B).

Theorem 1. *Let $\hat{\chi}(h, S) = \frac{1}{|S|} \sum_{x \in S} \chi(h, x)$ be the empirical compatibility over unlabeled dataset S . Let $\mathcal{H}_0 = \{h \in \mathcal{H} : \widehat{\text{err}}(h) = 0\}$. If $c^* \in \mathcal{H}$ and $\chi(c^*, P) = 1 - t$, then m_u unlabeled data and m_l labeled data are sufficient to learn to error ϵ with probability $1 - \delta$, for*

$$m_u = \mathcal{O} \left(\frac{VC\dim(\chi(\mathcal{H}))}{\epsilon^2} \log \frac{1}{\epsilon} + \frac{1}{\epsilon^2} \log \frac{2}{\delta} \right) \quad (1)$$

and

$$m_l = \frac{2}{\epsilon} \left[\ln(2\mathcal{H}_{P,\chi}(t + 2\epsilon)[2m_l, P]) + \ln \frac{4}{\delta} \right], \quad (2)$$

where $\chi(\mathcal{H}) = \{\chi_h : h \in \mathcal{H}\}$, $\chi_h(\cdot) = \chi(h, \cdot)$, and $\mathcal{H}_{P,\chi}(t + 2\epsilon)[2m_l, P]$ is the expected number of splits of $2m_l$ data drawn from P using hypotheses in \mathcal{H} of compatibility more than $1 - t - 2\epsilon$. In particular, with probability at least $1 - \delta$, we have $\text{err}(\hat{h}) \leq \epsilon$, where

$$\hat{h} = \arg \max_{h \in \mathcal{H}_0} \hat{\chi}(h, S). \quad (3)$$

Remark 1. If unlabeled data are highly compatible to c^* , t is small, which results in a smaller m_l . Namely, with the smaller m_l , we can still achieve a low error rate. In view of Theorem 1, it is clear that SSL will be learnable if many compatible unlabeled data are available. Motivated by SSL, we wonder if we can generate compatible data to help our learning task. The answer is *affirmative*.

Solving FHA in Principle. Motivated by Theorem 1, finding many highly compatible unlabeled data is a breakthrough point for FHA. Hence, generating unlabeled target data is a straightforward solution. However, due to the shortage of existing target data, directly generating them is unrealistic. To solve this problem, we can ask for help from the source classifier. In our paper, we first try to generate intermediate domain P_m containing knowledge of source and target domains, which are compatible with both source classifier and target classifier, i.e.,

$$P_m = \arg \max_P [\chi(h_s, P) + \chi(h_t, P)], \quad (4)$$

where $\chi(h_s, P)$ (resp. $\chi(h_t, P)$) measures how compatible h_s (resp. h_t) is with unlabeled data distribution P . Then, we will adapt intermediate domain P_m to the target domain via distributional adaptation with the training procedure going on. Finally, we can obtain many unlabeled data that is compatible with h_s and h_t (more compatible with h_t), meaning that, based on Theorem 1, we can address FHA in principle. According to Eq. (4), it can be seen that we can have two straightforward solutions: maximizing $\chi(h_s, P)$ or $\chi(h_t, P)$, corresponding to S+FADA and T+FADA in benchmark solutions. The results in Table 1 and Table 2 indicate that these two straightforward solutions cannot address FHA well, which motivate us to maximize them simultaneously, which is realized below.

4 Target Orientated Hypothesis Adaptation Network for FHA Problem

In this section, we propose a powerful one-step approach: *target orientated hypothesis adaptation network* (TOHAN, see Figure 2). TOHAN can generate data that are highly compatible with both source classifier and target classifier and adapt the knowledge of these data to target domain gradually.

Intermediate domain generation. The first step of TOHAN is to generate intermediate domain data (see Figure 2a). We input Gaussian random noise z to a generator G_n (taking the n^{th} class for an example), then the generator outputs the generated data. We aim to generate data satisfying two conditions: (1) the generated data $G_n(z)$ can be correctly classified by the given source classifier $f_s = h_s \circ g_s$, and (2) $G_n(z)$ becomes closer to target domain with training procedure going on. Thus, there are two loss functions regarding to the intermediate domain generation. The first one is introduced below.

Without loss of the generality, we assume $G_n(z)$ generates B images, where B is the batchsize in the training process of TOHAN. When $G_n(z)$ is inputted to the source-domain classifier f_s , we will obtain an $B \times N$ matrix \mathbf{G}_n^M , where the i^{th} row in \mathbf{G}_n^M represents probability of the i^{th} generated image belonging to each class. Thus, the n^{th} column in \mathbf{G}_n^M represents the probability that the B generated images belongs to the n^{th} class, and we denote the n^{th} column in \mathbf{G}_n^M as l_n . Since $G_n(z)$ aims to generate data belonging to the n^{th} class, we should update parameters of \mathbf{G}_n^M to make each element in l_n close to 1. Namely, the first loss function to train the G_n can be defined as

$$\mathcal{L}_{G_n}^s = \frac{1}{B} \|l_n - \mathbb{1}\|_2^2, \quad (5)$$

where $\mathbb{1}$ is a B -by-1 vector whose elements are 1.

As discussed before, we also want to reduce the distance between the generated data $G_n(z)$ and the target data whose labels are n . In this way, we can make the generated data close to the target domain and attain an intermediate domain \mathcal{D}_m . Following [22], we adopt an augmented L_1 distance $\|X - Y\|_1 = \sum_i \omega_i |X_i - Y_i|$, where $\omega_i = |X_i - Y_i|^2 / \|X - Y\|_2$. Compared to ordinary ℓ_1 norm, the augmented L_1 distance encourages larger gradients for feature dimensions with higher residual error [22]. Compared to the ℓ_2 norm, since L_1 distance is more robust to outliers [30], it is better to measure the distance between generated images and target images. Thus, the second loss to train G_n is defined as follows,

$$\mathcal{L}_{G_n}^t = \frac{1}{MBK} \sum_{i=1}^B \sum_{k=1}^K \|x_m^i - x_t^k\|_1, \quad (6)$$

where $M = \max_{x_1, x_2 \in \mathcal{X}} \|x_1 - x_2\|_1$ (\mathcal{X} is compact and $\|\cdot\|_1$ is continuous) and $G_n(z) := \{x_m^i\}_{i=1}^B$. Combining Eq. (5) and Eq. (6), we obtain the total loss to train the generator G_n :

$$\mathcal{L}_{G_n} = \mathcal{L}_{G_n}^s + \lambda \mathcal{L}_{G_n}^t = \frac{1}{B} \|l_n - \mathbb{1}\|_2^2 + \frac{\lambda}{MBK} \sum_{i=1}^B \sum_{k=1}^K \|x_m^i - x_t^k\|_1, \quad (7)$$

where λ is a hyper-parameter between two losses to tradeoff the weight of knowledge of source-domain and target-domain. To ensure that generated data are high-quality images, we train the generator G_n ($n = 1, \dots, N$) for some steps all alone. And we claim that optimizing Eq. (7) is corresponding to Eq. (4). More specifically, Eq (5) (resp. Eq. (6)) is corresponding to $\chi(h_s, P_m)$ (resp. $\chi(h_t, P_m)$). Then we conduct intermediate-to-target distributional adaptation (see the next paragraph) and generation simultaneously.

Intermediate-to-target distributional adaptation. Now, we focus on how to construct *domain-invariant representations* (DIP) between the intermediate domain and the target domain. Through DIP, classifier for the intermediate domain can be used to classify target data well.

Since we only have few target data per class, so we aim to “augment” them. Following [28], we can overcome the shortage of target data by pairing them with corresponding intermediate data. Specifically, we create 4 groups of data pairs: \mathcal{G}_1 consists of data pairs from the intermediate domain with the same label, \mathcal{G}_2 consists of pairs from different domains (one from the intermediate and one from the target domain) but with the same label, \mathcal{G}_3 consists of pairs from the same domain with different labels, and \mathcal{G}_4

consists of pairs from different domains (one from the intermediate and one from the target domain) and with different labels.

Based on the above four groups, we construct a four-class group discriminator D to decide which of the four groups a given data pair belongs to, which differs from classical adversarial domain adaptation [9, 15]. The group discriminator D aims to classify the data pair groups. As a classification problem, we train D with the standard categorical cross-entropy loss:

$$\mathcal{L}_D = -\hat{\mathbb{E}} \left[\sum_{i=1}^4 y_{\mathcal{G}_i} \log (D(\phi(\mathcal{G}_i))) \right], \quad (8)$$

where $\hat{\mathbb{E}}[\cdot]$ represents the empirical mean value, $y_{\mathcal{G}_i}$ is the label of group \mathcal{G}_i , and $\phi(\mathcal{G}_i) := [g_t(x_1), g_t(x_2)]$, $(x_1, x_2) \in \mathcal{G}_i$, and g_t is the encoder on target domain. Note that we will freeze g_t when minimizing the above loss function (see Figure 2b).

Next, we turn to train g_t and h_t with the group discriminator D fixed, which confuses D unable to distinguish between \mathcal{G}_1 and \mathcal{G}_2 (also \mathcal{G}_3 and \mathcal{G}_4). However, we need D to correctly discriminate positive pairs ($\mathcal{G}_1, \mathcal{G}_2$) from negative pairs ($\mathcal{G}_3, \mathcal{G}_4$). This means that domain confusion and classification are realized at the same time. We firstly initial g_t and h_t with the same weight as g_s and h_s , respectively. Motivated by non-saturating game [10], we minimize the following loss to update g_t and h_t (see Figure 2c):

$$\mathcal{L}_{h \circ g} = -\beta \hat{\mathbb{E}} [y_{\mathcal{G}_1} \log (D(\phi(\mathcal{G}_2))) - y_{\mathcal{G}_3} \log (D(\phi(\mathcal{G}_4)))] + \hat{\mathbb{E}} [\ell(f_t(X_t), f_t^*(X_t))], \quad (9)$$

where β is a hyper-parameter to tradeoff confusion and classification and ℓ is the cross-entropy loss. $f_t := g_t \circ h_t$ is the target model and f_t^* is the optimal target model. Corresponding to Theorem 1, optimizing the first term in Eq. (9) increases compatibility of target classifier with intermediate data, and optimizing the second term in Eq. (9) reduces $\hat{err}(h_t)$, resulting in a smaller $err(h_t)$. Compared to [28], Eq. (9) means that we train target-domain classifier by confusing D and improving classification accuracy simultaneously.

TOHAN: A one-step solution to FHA. Although we can sequentially combine the above two steps to solve the FHA problem (i.e., a two-step solution), the fixed intermediate domain (generated by the first step) may have large distributional discrepancy with target domain. As a result, such two-step solution may not obtain a good target-domain classifier. To address this issue, we introduce a one-step solution TOHAN. The ablation study verifies that TOHAN outperforms such two-step solution (see ST+F and TOHAN in Table 3).

The entire training procedures of TOHAN are shown in Algorithm 1. Since the convergence speed of generator G is relatively slow, the quality of generated data is poor at the beginning of the training process of G . Thus, we will train the generator G for certain epochs before doing intermediate-to-target distributional adaptation (lines 2 to 5). When the generator can generate high-quality images, we will train the generator and conduct adaptation altogether.

We train every generator G_n ($n = 1, 2, \dots, N$) separately, and we generate intermediate domain data using the latest generators. Then, we pair intermediate data with target data and pre-train the group discriminator D (lines 6 to 8). Next, we pair the intermediate data with target data and conduct the adaptation (lines 9 to 12). After conducting intermediate-to-target distributional adaptation, we will obtain better g_t and h_t , i.e. classifying the intermediate domain data more accurately. With the better target-domain classifier, we can make the generated intermediate data get closer to the target domain, in turn, these generated intermediate data furthermore promote the adaptation performance.

Why does TOHAN prevent the leakage of private information effectively? As mentioned above, TOHAN generates intermediate domain data containing knowledge of source domain and target

Algorithm 1 Target orientated hypothesis adaptation network (TOHAN)

Input: encoder g_s , classifier h_s , $D_t = \{x_t^i, y_t^i\}_{i=1}^{n_t}$, learning rate $\gamma_1, \gamma_2, \gamma_3$ and γ_4 , total epoch T_{max} , pretraining D epoch T_d , adaptation epoch T_f , network parameter $\{\theta_{G_n}\}_{n=1}^N, \theta_{hog}, \theta_D$.

1: Initialize $\{\theta_{G_n}\}_{n=1}^N$ and θ_D ;

for $t = 1, 2, \dots, T_{max}$ **do**

2: Initialize $\mathcal{D}_m = \emptyset$

for $n = 0, 1, \dots, N - 1$ **do**

3: Generate random noise z ;

4: Generate data $G_n(z)$ then add them to \mathcal{D}_m

5: Update $\theta_{G_n} \leftarrow \theta_{G_n} - \gamma_1 \nabla \mathcal{L}_{G_n}(z, D_t)$ using Eq. (7);

end

if $t = T_{max} - T_f$ **then**

for $i = 1, 2, \dots, T_d$ **do**

6: Sample $\mathcal{G}_1, \mathcal{G}_3$ from $\mathcal{D}_m \times \mathcal{D}_m$;

7: Sample $\mathcal{G}_2, \mathcal{G}_4$ from $\mathcal{D}_m \times \mathcal{D}_t$;

8: Update $\theta_D \leftarrow \theta_D - \gamma_2 \nabla \mathcal{L}_D(\{\mathcal{G}_i\}_{i=1}^4)$ using Eq. (8);

end

end

if $t \geq T_{max} - T_f$ **then**

9: Sample $\mathcal{G}_1, \mathcal{G}_3$ from $\mathcal{D}_m \times \mathcal{D}_m$;

10: Sample $\mathcal{G}_2, \mathcal{G}_4$ from $\mathcal{D}_m \times \mathcal{D}_t$;

11: Update $\theta_{hog} \leftarrow \theta_{hog} - \gamma_3 \mathcal{L}_{hog}(\{\mathcal{G}_i\}_{i=1}^4, x_m, x_t)$ using Eq. (9);

12: Update $\theta_D \leftarrow \theta_D - \gamma_4 \nabla \mathcal{L}_D(\{\mathcal{G}_i\}_{i=1}^4)$ using Eq. (8);

end

end

Output: the neural network $h_t \circ g_t$.

domain. The knowledge of source domain is mainly the underlying features, dominating which class an intermediate data belongs to. However, the high-level, visual and useful features of source domain are rare in the generated intermediate data (Figure 4). Thus, it is clear that the high-level features of intermediate data mostly come from target domain. Therefore, the useful knowledge of the source domain is completely unaccessible. Therefore, the privacy information in the source domain is protected strictly.

5 Experiments

In this section, we compare TOHAN with possible benchmark solutions on five standard supervised DA datasets: *MNIST*(*M*), *SYHN*(*S*), *USPS*(*U*), *CIFAR-10*(*CF*), *STL-10*(*SL*). We follow the standard domain-adaptation protocols [34] and compare average accuracy of 5 independent repeated experiments. For digital datasets (i.e., *M*, *S*, and *U*), we choose the number of target data from 1 to 7 following [28]. For objective datasets (i.e., *CF* and *SL*), we choose the number of target data as 10. Details regarding these datasets can be found in Appendix C.

Benchmark solutions for FHA. Although the FHA is a new problem setting, we still design 5 benchmark solutions to this new problem. (1) *Without adaptation* (WA): to classify target domain with the source classifier (encoder g_s and classifier h_s). (2) *Fine tuning* (FT): to train the classifier g_s with few owned target data. (3) *SHOT*: a novel HTL method, where we modify it to use labeled target data instead of only using unlabeled target data. [21]. (4) *S+FADA* (S+F): to generate fake source data with the source classifier then apply them into DANN [9]. (5) *T+FADA* (T+F): to generate fake target data with few real target data then apply them into DANN. We demonstrate details of 5 benchmark solutions

Table 1: Classification accuracy \pm standard deviation (%) on 6 digits FHA tasks. Bold value represents the highest accuracy on each column.

Tasks	WA	FHA Methods	Number of Target Data per Class						
			1	2	3	4	5	6	7
$M \rightarrow S$	24.1	FT	26.7 \pm 1.0	26.8 \pm 2.1	26.8 \pm 1.6	27.0 \pm 0.7	27.3 \pm 1.2	27.5 \pm 0.8	28.3 \pm 1.5
		SHOT	25.7 \pm 2.2	26.9 \pm 1.2	27.9 \pm 2.6	29.1 \pm 0.4	29.1 \pm 1.4	29.6 \pm 1.7	29.8 \pm 1.5
		S+F	25.6 \pm 1.3	27.7 \pm 0.5	27.8 \pm 0.7	28.2 \pm 1.3	28.4 \pm 1.4	29.0 \pm 1.0	29.6 \pm 1.9
		T+F	25.3 \pm 1.0	26.3 \pm 0.8	28.9 \pm 1.0	29.1 \pm 1.3	29.2 \pm 1.3	31.9 \pm 0.4	32.4 \pm 1.8
		TOHAN	26.7\pm0.1	28.6\pm1.1	29.5\pm1.4	29.6\pm0.4	30.5\pm1.2	32.1\pm0.2	33.2\pm0.8
$S \rightarrow M$	70.2	FT	70.2 \pm 0.0	70.6 \pm 0.3	70.7 \pm 0.1	70.8 \pm 0.3	70.9 \pm 0.2	71.1 \pm 0.3	71.1 \pm 0.4
		SHOT	72.6 \pm 1.9	73.6 \pm 2.0	74.1 \pm 0.6	74.6 \pm 1.2	74.9 \pm 0.7	75.4 \pm 0.3	76.1 \pm 1.5
		S+F	74.4 \pm 1.5	83.1 \pm 0.7	83.3 \pm 1.1	85.9 \pm 0.5	86.0 \pm 1.2	87.6 \pm 2.6	89.1 \pm 1.0
		T+F	74.2 \pm 1.8	81.6 \pm 4.0	83.4 \pm 0.8	82.0 \pm 2.3	86.2 \pm 0.7	87.2 \pm 0.8	88.2 \pm 0.6
		TOHAN	76.0\pm1.9	83.3\pm0.3	84.2\pm0.4	86.5\pm1.1	87.1\pm1.3	88.0\pm0.5	89.7\pm0.5
$M \rightarrow U$	69.7	FT	74.4 \pm 0.7	76.7 \pm 1.9	76.9 \pm 2.2	77.3 \pm 1.1	77.6 \pm 1.4	78.3 \pm 2.1	78.3 \pm 1.6
		SHOT	87.2 \pm 0.2	87.9 \pm 0.3	87.8 \pm 0.4	88.0 \pm 0.4	87.9 \pm 0.5	88.0 \pm 0.3	88.4 \pm 0.3
		S+F	83.7 \pm 0.9	86.0 \pm 0.4	86.1 \pm 1.1	86.5 \pm 0.8	86.8 \pm 1.4	87.0 \pm 0.6	87.2 \pm 0.8
		T+F	84.2 \pm 0.1	84.2 \pm 0.3	85.2 \pm 0.9	85.2 \pm 0.6	86.0 \pm 1.5	86.8 \pm 1.5	87.2 \pm 0.5
		TOHAN	87.7\pm0.7	88.3\pm0.5	88.5\pm1.2	89.3\pm0.9	89.4\pm0.8	90.0\pm1.0	90.4\pm1.2
$U \rightarrow M$	82.9	FT	83.5 \pm 0.4	84.3 \pm 2.4	84.5 \pm 0.7	85.5 \pm 1.3	86.6 \pm 1.0	87.2 \pm 0.7	88.1 \pm 2.7
		SHOT	83.1 \pm 0.5	85.5\pm0.3	85.8\pm0.6	86.0 \pm 0.2	86.6 \pm 0.2	86.7 \pm 0.2	87.0 \pm 0.1
		S+F	83.2 \pm 0.2	84.0 \pm 0.3	85.0 \pm 1.2	85.6 \pm 0.5	85.7 \pm 0.6	86.2 \pm 0.6	87.2 \pm 1.1
		T+F	82.9 \pm 0.7	83.9 \pm 0.2	84.7 \pm 0.8	85.4 \pm 0.6	85.6 \pm 0.7	86.3 \pm 0.9	86.6 \pm 0.7
		TOHAN	84.0\pm0.5	85.2 \pm 0.3	85.6 \pm 0.7	86.5\pm0.5	87.3\pm0.6	88.2\pm0.7	89.2\pm0.5
$S \rightarrow U$	64.3	FT	64.9 \pm 1.1	66.5 \pm 1.5	66.7 \pm 1.7	67.3 \pm 1.1	68.1 \pm 2.3	68.3 \pm 0.5	69.7 \pm 1.4
		SHOT	74.7 \pm 0.3	75.5 \pm 1.4	75.6 \pm 1.0	75.8 \pm 0.7	77.1 \pm 2.1	77.8 \pm 1.6	79.6 \pm 0.6
		S+F	72.2 \pm 1.4	73.6 \pm 1.4	74.7 \pm 1.4	76.2 \pm 1.3	77.2 \pm 1.7	77.8 \pm 3.0	79.7 \pm 1.9
		T+F	71.7 \pm 0.6	74.3 \pm 1.9	74.5 \pm 0.8	75.9 \pm 2.1	77.7 \pm 1.5	76.8 \pm 1.8	79.7 \pm 1.9
		TOHAN	75.8\pm0.9	76.8\pm1.2	79.4\pm0.9	80.2\pm0.6	80.5\pm1.4	81.1\pm1.1	82.6\pm1.9
$U \rightarrow S$	17.3	FT	23.4 \pm 1.8	23.6 \pm 2.7	23.8 \pm 1.6	24.6 \pm 1.4	24.6 \pm 1.2	24.8 \pm 0.7	25.5 \pm 1.8
		SHOT	30.3\pm1.2	31.6\pm0.4	29.8 \pm 0.5	29.4 \pm 0.3	29.7 \pm 0.5	29.8 \pm 0.8	30.1 \pm 0.9
		S+F	28.1 \pm 1.2	28.7 \pm 1.3	29.0 \pm 1.2	30.1 \pm 1.1	30.3 \pm 1.3	30.7 \pm 1.0	30.9 \pm 1.5
		T+F	27.5 \pm 1.4	27.9 \pm 0.9	28.4 \pm 1.3	29.4 \pm 1.8	29.5 \pm 0.7	30.2 \pm 1.0	30.4 \pm 1.7
		TOHAN	29.9 \pm 1.2	30.5 \pm 1.2	31.4\pm1.1	32.8\pm0.9	33.1\pm1.0	34.0\pm1.0	35.1\pm1.8

in Appendix D. Experimental details can be found in Appendix E. Moreover, we conduct additional experiments about existing HTL methods in Appendix F.

Results on digits FHA tasks. We conduct experiments on 6 digits FHA tasks: $M \rightarrow S$, $S \rightarrow M$, $M \rightarrow U$, $U \rightarrow M$, $S \rightarrow U$ and $U \rightarrow S$. Table 1 reports target-domain classification accuracy of 6 methods on 6 digits FHA tasks. It is clear that TOHAN performs the best on almost every tasks. On $M \rightarrow S$, $S \rightarrow M$, $M \rightarrow U$ and $S \rightarrow U$, TOHAN outperforms all benchmark solutions obviously. However, on the tasks of $U \rightarrow M$ and $U \rightarrow S$, the accuracy of TOHAN is slightly lower than SHOT when the amount of target data is too small ($n = 1, 2$). This abnormal phenomenon shows that TOHAN cannot generate intermediate domain data effectively with very little target data, especially when the resolution of source data is much smaller than that of target data. In this case, the data we generate is close to source domain, so TOHAN degrades to S+FADA.

In Appendix G, we use t-SNE to visualize the feature extracted by TOHAN and 5 benchmark solutions on $M \rightarrow U$ task (see Figure 7 in Appendix G). When we use WA and FT methods, nearly all classes mix together. Although the classification accuracy of SHOT, S+F and T+F are relatively high, there are still a little mixtures among classes. For TOHAN, it can be seen that all classes are separated well, which demonstrates that TOHAN works well for solving FHA problem.

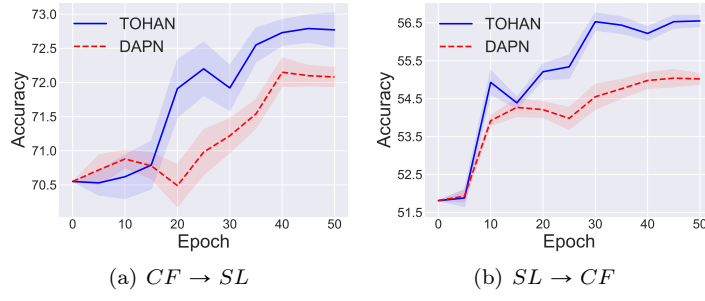


Figure 3: TOHAN vs DAPN.

Results on objects FHA tasks. Following [34], we also evaluate TOHAN and benchmark solutions on 2 objects FHA tasks: $SL \rightarrow CF$ and $CF \rightarrow SL$. Considering the complexity of datasets and the difficulty of our problem setting, we do not have amazing results like digits tasks. In $SL \rightarrow CF$, we achieve of 4.8% improvement over WA and a performance accuracy of 56.9%. Note that because the number of pixels per image of CF and SL are quite different, the images from SL will lose a lot of information when inputted to the pre-trained model of CF , thus making the effects of TOHAN and benchmark solutions are not obvious for $CF \rightarrow SL$.

Comparing TOHAN with FSL methods. As mentioned above, FHA is a difficult case of FSL where the prior knowledge is a pre-trained model of another domain. To test the effectiveness of FSL methods in FHA, we compare TOHAN with a novel FSL method called *domain-adaptive few-shot learning* (DAPN) [54]. Note that we use the same pre-trained model in both TOHAN and DAPN. Taking $CF \leftrightarrow SL$ with five target data (per class) as an example, we solve FHA with TOHAN and DAPN and show the results in Figure 3. It is clear that TOHAN outperforms DAPN when the training epoch (t) is relatively large.

Ablation Study. Finally, we study the advantages of one-step method over other two-step methods. We consider the following baselines: S+F, T+F and *ST+FADA* (ST+F). We have explained S+F and T+F previously. ST+F denotes the two-step version of TOHAN, i.e., to conduct intermediate domain generation and intermediate-to-target distributional adaptation separately. We make ablation study on three digital datasets mentioned before as an example.

As shown in Table 3, it is clear that TOHAN works better than other baselines. The generator of S+F uses the loss $\mathcal{L}_{G_n}^s$, which merely contains knowledge from source domain. The generator of T+F uses the loss $\mathcal{L}_{G_n}^t$ and ignores the knowledge contained in the source-domain classifier. Compared to them, TOHAN uses both $\mathcal{L}_{G_n}^s$ and $\mathcal{L}_{G_n}^t$. As a result, TOHAN achieves higher accuracy than S+F and T+F. Besides, generators and classifiers in TOHAN will promote each other in the training process, which results in that TOHAN performs better than the ST+F. In Figure 4, we visualize the data generated by S+FADA and TOHAN. It is clear that data generated by S+FADA are chaotic that contain little useful information. However, data generated by TOHAN contain many target domain high-level and visual features, and they can be classified by source classifier accurately, resulting in a better performance in FHA. The detailed analysis of ablation study can be found in Appendix G.

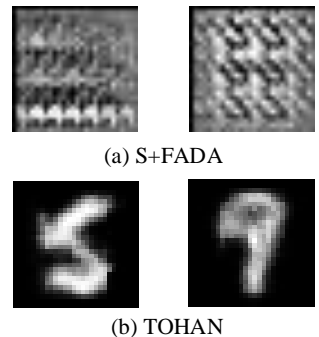


Figure 4: Visualization of S+FADA and TOHAN.

Table 2: Classification accuracy \pm standard deviation (%) on 2 objects FHA tasks: CIFAR-10 \rightarrow STL-10 ($CF \rightarrow SL$) and STL-10 \rightarrow CIFAR-10 ($SL \rightarrow CF$). Bold value represents the highest accuracy (%) among TOHAN and benchmark solutions.

Methods	WA	FT	SHOT	S+F	T+F	TOHAN
$CF \rightarrow SL$	70.6	71.5 ± 1.0	71.9 ± 0.4	72.1 ± 0.4	71.3 ± 0.5	72.8 ± 0.1
$SL \rightarrow CF$	51.8	54.3 ± 0.5	53.9 ± 0.2	56.9 ± 0.5	55.8 ± 0.8	56.6 ± 0.3

Table 3: Ablation study. We show the average accuracy of 6 tasks on digits datasets in this table. Bold value represents the highest accuracy (%) on each column. See full results in Appendix G.

Methods	FHA						
	Number of Target Data per Class						
	1	2	3	4	5	6	7
S+F	61.2	63.0	64.3	65.4	65.7	66.4	67.2
T+F	61.0	63.0	64.2	64.5	65.7	66.5	67.4
ST+F	61.8	64.5	64.9	65.8	66.5	67.3	68.4
TOHAN	63.3	65.4	66.4	67.5	68.0	68.9	70.0

6 Conclusion

This paper presents a very challenging problem setting called *few-shot hypothesis adaptation* (FHA), which trains a target-domain classifier with only few labeled target data and a well-trained source-domain classifier. Since we can only access a well-trained source-domain classifier in FHA, the private information in the source domain will be protected well. To this end, we propose a novel one-step FHA method, called *target orientated hypothesis adaptation network* (TOHAN). Experiments conducted on 8 FHA tasks confirm that TOHAN effectively adapts the source-domain classifier to the target domain and outperforms competitive benchmark solutions to the FHA problem.

References

- [1] Sk Miraj Ahmed, Aske R. Lejbølle, Rameswar Panda, and Amit K. Roy-Chowdhury. Camera on-boarding for person re-identification using hypothesis transfer learning. In *CVPR*, pages 12141–12150, 2020.
- [2] Sercan Ömer Arik, Jitong Chen, Kainan Peng, Wei Ping, and Yanqi Zhou. Neural voice cloning with a few samples. In *NeurIPS*, 2018.
- [3] Adam Coates, Andrew Ng, and Honglak Lee. An Analysis of Single Layer Networks in Unsupervised Feature Learning. In *AISTATS*, 2011.
- [4] Luc Devroye, László Györfi, and Gábor Lugosi. *A Probabilistic Theory of Pattern Recognition*. Springer, 1996.
- [5] Harrison Edwards and Amos J. Storkey. Towards a neural statistician. In *ICLR*, 2017.
- [6] Tongtong Fang, Nan Lu, Gang Niu, and Masashi Sugiyama. Rethinking importance weighting for deep learning under distribution shift. In *NeurIPS*, 2020.

- [7] Zhen Fang, Jie Lu, Feng Liu, Junyu Xuan, and Guangquan Zhang. Open set domain adaptation: Theoretical bound and algorithm. *IEEE Transactions on Neural Networks and Learning Systems*, 2020.
- [8] Chelsea Finn, Pieter Abbeel, and Sergey Levine. Model-agnostic meta-learning for fast adaptation of deep networks. In *ICML*, 2017.
- [9] Y. Ganin, E. Ustinova, H. Ajakan, P. Germain, H. Larochelle, F. Laviolette, M. Marchand, and V. Lempitsky. Domain-adversarial training of neural networks. *Journal of Machine Learning Research*, 17(59):1–35, 2016.
- [10] Ian Goodfellow. Neurips 2016 tutorial: Generative adversarial networks. *arXiv preprint arXiv:1701.00160*, 2016.
- [11] Yunzhong Hou and Liang Zheng. Source free domain adaptation with image translation. *arXiv preprint arXiv:2008.07514*, 2020.
- [12] Gao Huang, Zhuang Liu, Laurens Van Der Maaten, and Kilian Q Weinberger. Densely connected convolutional networks. In *CVPR*, 2017.
- [13] Jonathan J. Hull. A database for handwritten text recognition research. *IEEE Trans. Pattern Anal. Mach. Intell.*, 16(5):550–554, 1994.
- [14] Bargav Jayaraman and David Evans. Evaluating differentially private machine learning in practice. In *USENIX*, 2019.
- [15] Pin Jiang, Aming Wu, Yahong Han, Yunfeng Shao, Meiyu Qi, and Bingshuai Li. Bidirectional adversarial training for semi-supervised domain adaptation. In *IJCAI*, 2020.
- [16] Yongcheng Jing, Xiao Liu, Yukang Ding, Xinchao Wang, Errui Ding, Mingli Song, and Shilei Wen. Dynamic instance normalization for arbitrary style transfer. In *AAAI*, 2020.
- [17] Alex Krizhevsky, Geoffrey Hinton, et al. Learning multiple layers of features from tiny images. *Technical Report*, 2009.
- [18] Jogendra Nath Kundu, Naveen Venkat, R Venkatesh Babu, et al. Universal source-free domain adaptation. In *CVPR*, 2020.
- [19] Ilja Kuzborskij and Francesco Orabona. Stability and hypothesis transfer learning. In *ICML*, 2013.
- [20] Yann LeCun, Léon Bottou, Yoshua Bengio, and Patrick Haffner. Gradient-based learning applied to document recognition. *Proceedings of the IEEE*, 86(11):2278–2324, 1998.
- [21] Jian Liang, Dapeng Hu, and Jiashi Feng. Do we really need to access the source data? source hypothesis transfer for unsupervised domain adaptation. In *ICML*, 2020.
- [22] Tsung-Yi Lin, Priya Goyal, Ross Girshick, Kaiming He, and Piotr Dollár. Focal loss for dense object detection. In *ICCV*, 2017.
- [23] F. Liu, J. Lu, B. Han, G. Niu, G. Zhang, and M. Sugiyama. Butterfly: A panacea for all difficulties in wildly unsupervised domain adaptation. In *NeurIPS LTS Workshop*, 2019.
- [24] Lu Liu, William Hamilton, Guodong Long, Jing Jiang, and Hugo Larochelle. A universal representation transformer layer for few-shot image classification. In *ICLR*, 2021.

[25] Lu Liu, Tianyi Zhou, Guodong Long, Jing Jiang, Lina Yao, and Chengqi Zhang. Prototype propagation networks (PPN) for weakly-supervised few-shot learning on category graph. In *IJCAI*, 2019.

[26] M. Long, Z. Cao, J. Wang, and M.I Jordan. Conditional adversarial domain adaptation. In *NeurIPS*, 2018.

[27] Nikhil Mishra, Mostafa Rohaninejad, Xi Chen, and Pieter Abbeel. A simple neural attentive meta-learner. In *ICLR*, 2018.

[28] Saeid Motiian, Quinn Jones, Seyed Iranmanesh, and Gianfranco Doretto. Few-shot adversarial domain adaptation. In *NeurIPS*, 2017.

[29] Yuval Netzer, Tao Wang, Adam Coates, Alessandro Bissacco, Bo Wu, and Andrew Y Ng. Reading digits in natural images with unsupervised feature learning. In *NeurIPS*, 2011.

[30] Feiping Nie, Heng Huang, Xiao Cai, and Chris H. Q. Ding. Efficient and robust feature selection via joint 2, 1-norms minimization. In *NeurIPS*, 2010.

[31] Luca Oneto, Michele Donini, Giulia Luise, Carlo Ciliberto, Andreas Maurer, and Massimiliano Pontil. Exploiting MMD and Sinkhorn divergences for fair and transferable representation learning. In *NeurIPS*, 2020.

[32] Seonwook Park, Shalini De Mello, Pavlo Molchanov, Umar Iqbal, Otmar Hilliges, and Jan Kautz. Few-shot adaptive gaze estimation. In *ICCV*, 2019.

[33] Alec Radford, Luke Metz, and Soumith Chintala. Unsupervised representation learning with deep convolutional generative adversarial networks. In *ICLR*, 2015.

[34] Rui Shu, Hung H. Bui, Hirokazu Narui, and Stefano Ermon. A DIRT-T approach to unsupervised domain adaptation. In *ICLR*, 2018.

[35] Jake Snell, Kevin Swersky, and Richard S. Zemel. Prototypical networks for few-shot learning. In *NeurIPS*, 2017.

[36] Jie Song, Yixin Chen, Xinchao Wang, Chengchao Shen, and Mingli Song. Deep model transferability from attribution maps. In *NeurIPS*, pages 6179–6189, 2019.

[37] Jie Song, Yixin Chen, Jingwen Ye, Xinchao Wang, Chengchao Shen, Feng Mao, and Mingli Song. DEPARA: deep attribution graph for deep knowledge transferability. In *CVPR*, 2020.

[38] S. Sukhija, N.C. Krishnan, and G. Singh. Supervised heterogeneous domain adaptation via random forests. In *IJCAI*, 2016.

[39] Qianru Sun, Yaoyao Liu, Tat-Seng Chua, and Bernt Schiele. Meta-transfer learning for few-shot learning. In *CVPR*, 2019.

[40] Takeshi Teshima, Issei Sato, and Masashi Sugiyama. Few-shot domain adaptation by causal mechanism transfer. In *ICML*, 2020.

[41] Vladimir N. Vapnik. *Statistical Learning Theory*. Wiley, 1998.

[42] Dong Wang, Yuan Zhang, Kexin Zhang, and Liwei Wang. Focalmix: Semi-supervised learning for 3d medical image detection. In *CVPR*, 2020.

- [43] Limin Wang, Yuanjun Xiong, Zhe Wang, Yu Qiao, Dahua Lin, Xiaoou Tang, and Luc Van Gool. Temporal segment networks for action recognition in videos. *IEEE Trans. Pattern Anal. Mach. Intell.*, 41(11):2740–2755, 2019.
- [44] Yaqing Wang, Quanming Yao, James T. Kwok, and Lionel M. Ni. Generalizing from a few examples: A survey on few-shot learning. *ACM Comput. Surv.*, 53(3):63:1–63:34, 2020.
- [45] Ying Wei, Yu Zhang, Junzhou Huang, and Qiang Yang. Transfer learning via learning to transfer. In *ICML*, 2018.
- [46] Chao Yang and Ser-Nam Lim. One-shot domain adaptation for face generation. In *CVPR*, 2020.
- [47] Shuo Yang, Lu Liu, and Min Xu. Free lunch for few-shot learning: Distribution calibration. In *ICLR*, 2021.
- [48] Xiyu Yu, Tongliang Liu, Mingming Gong, Kun Zhang, Kayhan Batmanghelich, and Dacheng Tao. Label-noise robust domain adaptation. In *ICML*, 2020.
- [49] Yiqin Yu, Xu Min, Shiwan Zhao, Jing Mei, Fei Wang, Dongsheng Li, Kenney Ng, and Shaochun Li. Dynamic knowledge distillation for black-box hypothesis transfer learning. *arXiv:2007.12355*, 2020.
- [50] Junyi Zhang, Ziliang Chen, Junying Huang, Liang Lin, and Dongyu Zhang. Few-shot structured domain adaptation for virtual-to-real scene parsing. In *ICCV*, 2019.
- [51] Kun Zhang, Mingming Gong, Petar Stojanov, Biwei Huang, QINGSONG LIU, and Clark Glymour. Domain adaptation as a problem of inference on graphical models. In *NeurIPS*, 2020.
- [52] Tianyi Zhang, Ikko Yamane, Nan Lu, and Masashi Sugiyama. A one-step approach to covariate shift adaptation. In *ACML*, 2020.
- [53] Yiyang Zhang, Feng Liu, Zhen Fang, Bo Yuan, Guangquan Zhang, and Jie Lu. Learning from a complementary-label source domain: Theory and algorithms. *IEEE Transactions on Neural Networks and Learning Systems*, 2021.
- [54] An Zhao, Mingyu Ding, Zhiwu Lu, Tao Xiang, Yulei Niu, Jiechao Guan, Ji-Rong Wen, and Ping Luo. Domain-adaptive few-shot learning. *arXiv preprint arXiv:2003.08626*, 2020.
- [55] Li Zhong, Zhen Fang, Feng Liu, Jie Lu, Bo Yuan, and Guangquan Zhang. How does the combined risk affect the performance of unsupervised domain adaptation approaches? *AAAI*, 2021.
- [56] Xiaojin Zhu. Semi-supervised learning. *Encyclopedia of Machine Learning*, pages 892–897, 2010.

A Related Work

In this section, we briefly review *few-shot learning* (FSL) and two domain adaptation settings related to the FHA problem, which include FDA, and *source-data-free UDA* (SFUDA).

Few-shot Learning. Existing FSL methods can be divided into three categories: (1) Augmenting training data set by prior knowledge. Data augmentation via hand-crafted rules serves as pre-processing in FSL methods. For instance, we can use reflection [5]; and (2) Constraining hypothesis space by prior knowledge [27]; and (3) Altering search strategy in hypothesis space by prior knowledge. For instance, we can use early-stopping [2]. Note that our method belongs to category (1). However, the prior knowledge we have is more difficult to leverage than the prior knowledge that FSL methods have.

Few-shot Domain Adaptation. With the development of FSL, researchers also apply ideas of FSL into domain adaptation, called *few-shot domain adaptation* (FDA). FADA [28] is a representative FDA method, which pairs data from source domain and data from target domain and then follows the adversarial domain adaptation method. Casual mechanism transfer [40] is another novel FDA method dealing with a meta-distributional scenario, in which the data generating mechanism is invariant among domains. Nevertheless, FDA methods still need to access many labeled source data for training, which may cause the private-information leakage of the source domain.

Hypothesis Transfer Learning. In the *hypothesis transfer learning* (HTL), we can only access a well-trained source-domain classifier and small labeled or abundant unlabeled target data. [19] requires small labeled target data and uses the Leave-One-Out error find the optimal transfer parameters. Later, SHOT [21] is proposed to solve the HTL with many unlabeled target data by freezing the source-domain classifier and learning a target-specific feature extraction module. [11] proposes an image translation method that transfers the style of target images to that of unseen source images. As for the universal setting, a two-stage learning process [18] has been proposed to address the HTL problem. Compared with FHA, HTL still requires at least small target data (e.g., at least 12 samples in binary classification problem [19], or at least two of labeling percentage [1]). In FHA, we focus on a more challenging situation: only few data (e.g., one sample per class) are available.

B Proof of Theorem 1

We state here two known generalization bounds [4] used in our proof.

Lemma 1. *Suppose that \mathcal{H} is a set of functions from \mathcal{X} to $\{0, 1\}$ with finite VC-dimension $V \geq 1$. For any distribution P over \mathcal{X} , any target function, and any $\epsilon, \delta > 0$, if we draw a set of data from P of size*

$$m(\epsilon, \delta, V) = \frac{64}{\epsilon^2} \left(2V \ln \left(\frac{12}{\epsilon} \right) + \ln \left(\frac{4}{\delta} \right) \right),$$

then with probability at least $1 - \delta$, we have $|\text{err}(h) - \widehat{\text{err}}(h)| \leq \epsilon$ for all $h \in \mathcal{H}$.

Lemma 2. *Suppose that \mathcal{H} is a set of functions from \mathcal{X} to $\{0, 1\}$ with finite VC-dimension $V \geq 1$. For any probability distribution P over \mathcal{X} , any target function c^* , we have*

$$\Pr \left[\sup_{h \in \mathcal{H}, \widehat{\text{err}}(h) = 0} |\text{err}(h) - \widehat{\text{err}}(h)| \geq \epsilon \right] \leq 2\mathcal{H}[2m, P]e^{-m\epsilon/2}.$$

So, for any $\epsilon, \delta > 0$, if we draw a set of data from P of size

$$m \geq \frac{2}{\epsilon} \left(2 \ln(\mathcal{H}[2m, P]) + \ln \left(\frac{2}{\delta} \right) \right),$$

then with probability at least $1 - \delta$, we have that all functions with $\widehat{\text{err}}(h) = 0$ satisfy

$$\text{err}(h) \leq \epsilon.$$

Now we begin the proof of Theorem 1.

Proof. Let S be the set of m_u unlabeled data. By standard VC-dimension bounds (e.g., Lemma 1), the number of unlabeled data given is sufficient to ensure that with probability at least $1 - \frac{\delta}{2}$ we have

$$|\mathbf{Pr}_{x \sim \bar{S}}[\chi_h(x) = 1] - \mathbf{Pr}_{x \sim P}[\chi_h(x) = 1]| \leq \epsilon \quad \text{for all } \chi_h \in \chi(\mathcal{H}).$$

Since $\chi_h(x) = \chi(h, x)$, this implies that we have

$$|\chi(h, D) - \hat{\chi}(h, S)| \leq \epsilon \quad \text{for all } h \in \mathcal{H}.$$

Therefore, the set of hypotheses with $\hat{\chi}(h, S) \geq 1 - t - \epsilon$ is contained in $\mathcal{H}_{P,\chi}(t + 2\epsilon)$.

The bound on the number of labeled data now follows directly from known concentration results using the expected number of partitions instead of the maximum in the standard VC-dimension bounds (e.g., Lemma 2). This bound ensures that with probability $1 - \frac{\delta}{2}$, none of the functions $h \in \mathcal{H}_{P,\chi}(t + 2\epsilon)$ with $\text{err}(h) \geq \epsilon$ have $\widehat{\text{err}}(h) = 0$.

The above two arguments together imply that with probability $1 - \delta$, all $h \in \mathcal{H}$ with $\widehat{\text{err}}(h) = 0$ and $\hat{\chi}(h, S) \geq 1 - t - \epsilon$ have $\text{err}(h) \geq \epsilon$, and furthermore c^* has $\hat{\chi}(c^*, S) \geq 1 - t - \epsilon$. This in turn implies that with probability at least $1 - \delta$, we have $\text{err}(\hat{h}) \leq \epsilon$, where

$$\hat{h} = \arg \max_{h \in \mathcal{H}_0} \hat{\chi}(h, S).$$

□

C Datasets

Digits. Following the evaluation protocol of [28], we conduct experiments on 6 adaptation scenarios: $M \rightarrow S$, $S \rightarrow M$, $M \rightarrow U$, $U \rightarrow M$, $S \rightarrow U$ and $U \rightarrow S$. MNIST [20] images have been size-normalized and centered in a fixed-size (28×28) image. USPS [13] images are 16×16 grayscale pixels. SVHN [29] images are 32×32 pixels with 3 channels.

Objects. We also evaluate TOHAN and benchmark solutions on CIFAR-10 [17] and STL-10 [3], following [34]. The CIFAR-10 dataset contains 60,000 32×32 color images in 10 categories. The STL-10 dataset is inspired by the CIFAR-10 dataset but with some modifications. However, these two datasets only contain nine overlapping classes. We removed the non-overlapping classes (“frog” and “monkey”) [34].

D Benchmark Solutions for FHA

To solve the FHA problem, this section presents 5 benchmark solutions that directly combine existing techniques used in the deep learning and domain adaptation fields.

Without adaptation. Since we have a source-domain classifier, we can directly use it to classify the target data, which is a frustrating solution to the FHA problem.

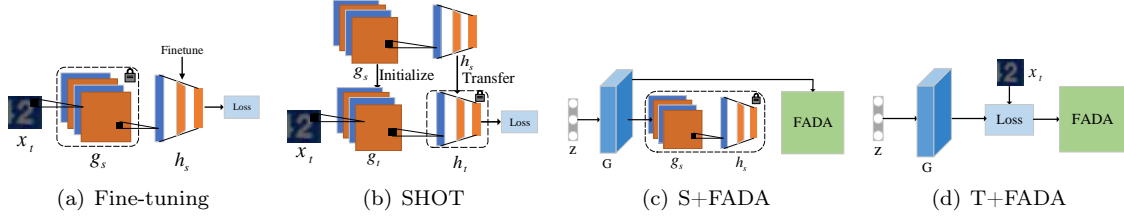


Figure 5: Overview of benchmark solutions to the FHA problem. (a) We freeze the source encoder g_s and train the source classifier h_s with the target data D_t . (b) We first train source encoder g_s and classifier h_s , then we transfer them to the target domain. We generate pseudo labels for target data, then we use them to train the target model with classifier h_t freezed. (c) We generate some source-like data under the guidance of the source classifier, then we combine them with FADA. (d) We generate some data close to target domain, i.e. decreasing the distance between data and target domain, then we combine them with FADA.

Fine-tuning. See Figure 5(a). Fine-tuning is a basic solution to the FHA problem. We freeze the source encoder g_s and train the source classifier h_s with the target data D_t . In this way, knowledge about target domain is filled into source hypothesis.

SHOT. See Figure 5(b). SHOT is a novel method for source hypothesis transfer [21]. It learns the optimal target-specific feature learning module to fit the source hypothesis with only the source classifier. We first train source encoder g_s and classifier h_s , and then we transfer them to the target domain. SHOT is an UDA method. Thus, we generate pseudo labels for target data, and then we use them to train the target model with classifier h_t freezed. Although SHOT is suitable for our FHA problem, it requires a lot of target data, which is an obstacle for FHA.

S+FADA. See Figure 5(c). As mentioned in Figure 6, a straightforward solution to the FHA problem is a two-step approach. We can train a source-data generator G under the guidance of source hypothesis, and then we use it to generate source data. First, we input Gaussian random noise z to G , then G outputs various disordered data. Second, these data is inputted into $g_s \circ h_s$, and then h_s outputs the probability of $G(z)$ belonging to each class. Third, if we would like to generate data belonging to n^{th} class, we should optimize G to push the probability of $G(z)$ belonging to n near to 1. Finally, we can apply the restored source data into an adversarial DA method to train a target domain classifier h_t .

T+FADA. See Figure 5(d). Different from S+FADA, here we train a generator with the help of target data instead, and then we will generate data close to target domain. We input Gaussian random noise z to generator G and minimize the distance between $G(z)$ and target data simultaneously. Finally, we sequentially combine these generated data with adversarial DA method to train a target-domain classifier.

E Implementation Details

We implement all methods by PyTorch 1.7.1 and Python 3.7.6, and conduct all the experiments on two NVIDIA RTX 2080Ti GPUs.

Network architecture. We select architecture of generators G_n ($n = 1, \dots, N$) from DCGAN [33]. For digits tasks, the encoder g , classifier h and group discriminator D share the same architecture in all 6 tasks, following FADA [28]. As for encoder g , we employ the backbone network of LeNet-5 with batch

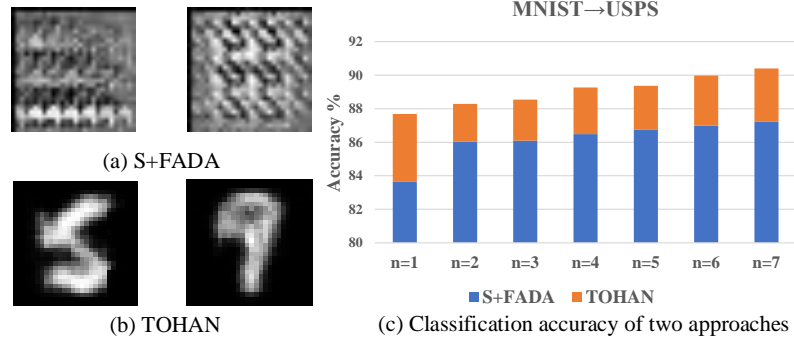


Figure 6: A straightforward solution for FHA is a two-step approach. Namely, we can first generate source data and then train a target-domain classifier using the generated source data and an FDA method (e.g., *few-shot adversarial domain adaptation* (FADA)). A visualized comparison between S+FADA and TOHAN (take MNIST → USPS as an example) is displayed in subfigures (a) and (b). On the left side, Subfigure (a) illustrates source-domain data generated by a two-step method: S+FADA. It is clear that the generated data are just noise and do not contain useful information about the source domain. In subfigure (b), we illustrate the intermediate-domain data generated by our method (i.e., TOHAN). It is clear that the generated intermediate-domain data contain useful information about two domains. In subfigure (c), the histogram shows classification accuracy of the two methods, and TOHAN outperforms S+FADA clearly.

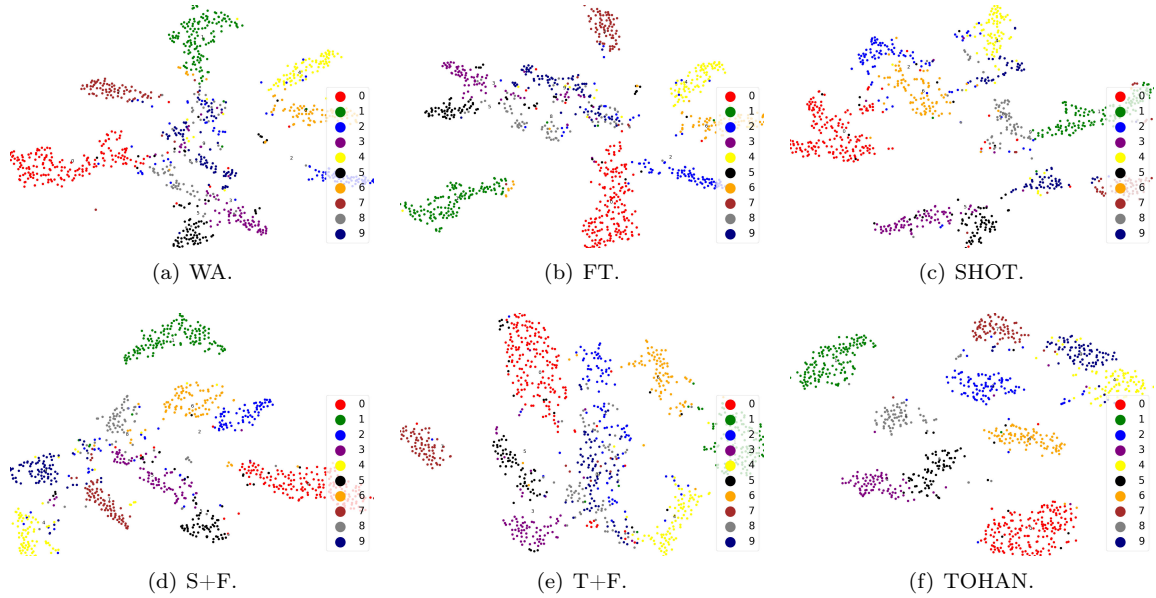


Figure 7: The t-SNE visualization for a 10-way classification task (taking *MNIST* → *USPS* as an example). When we use WA and FT methods, nearly all classes mix together. Although the classification accuracy of SHOT, S+F and T+F are relatively high, there are still a little mixtures among classes. For TOHAN, it can be seen that all classes are separated well. Namely, TOHAN works well for solving FHA problem.

Table 4: Comparison between dkdHTL and TOHAN. We report the classification accuracy \pm standard deviation (%) on 6 digits FHA tasks. Bold value represents the highest accuracy on each column.

Tasks	FHA Methods	Number of Target Data per Class						
		1	2	3	4	5	6	7
$M \rightarrow S$	dkdHTL	24.1 \pm 0.7	24.1 \pm 0.3	24.5 \pm 0.6	24.4 \pm 1.1	25.4 \pm 0.8	25.7 \pm 0.5	26.1 \pm 1.1
	TOHAN	26.7\pm0.1	28.6\pm1.1	29.5\pm1.4	29.6\pm0.4	30.5\pm1.2	32.1\pm0.2	33.2\pm0.8
$S \rightarrow M$	dkdHTL	71.2 \pm 1.2	83.4\pm0.4	88.5\pm0.6	88.2\pm0.7	89.5\pm0.7	89.6\pm0.4	90.3\pm0.2
	TOHAN	76.0\pm1.9	83.3 \pm 0.3	84.2 \pm 0.4	86.5 \pm 1.1	87.1 \pm 1.3	88.0 \pm 0.5	89.7 \pm 0.5
$M \rightarrow U$	dkdHTL	65.2 \pm 0.6	70.5 \pm 1.3	74.4 \pm 0.6	77.8 \pm 0.6	78.6 \pm 0.9	78.8 \pm 1.1	79.0 \pm 1.3
	TOHAN	87.7\pm0.7	88.3\pm0.5	88.5\pm1.2	89.3\pm0.9	89.4\pm0.8	90.0\pm1.0	90.4\pm1.2
$U \rightarrow M$	dkdHTL	83.2 \pm 0.2	85.5\pm0.5	85.9\pm0.4	85.7 \pm 0.8	86.2 \pm 0.2	86.2 \pm 0.4	86.8 \pm 0.3
	TOHAN	84.0\pm0.5	85.2 \pm 0.3	85.6 \pm 0.7	86.5\pm0.5	87.3\pm0.6	88.2\pm0.7	89.2\pm0.5
$S \rightarrow U$	dkdHTL	76.3\pm0.3	77.6\pm0.5	78.9 \pm 0.4	79.5 \pm 0.4	80.2 \pm 0.5	80.7 \pm 0.4	82.1 \pm 0.4
	TOHAN	75.8 \pm 0.9	76.8 \pm 1.2	79.4\pm0.9	80.2\pm0.6	80.5\pm1.4	81.1\pm1.1	82.6\pm1.9
$U \rightarrow S$	dkdHTL	20.5 \pm 0.8	20.9 \pm 0.4	21.7 \pm 0.3	23.8 \pm 0.2	24.5 \pm 0.7	25.5 \pm 0.6	25.7 \pm 0.4
	TOHAN	29.9\pm1.2	30.5\pm1.2	31.4\pm1.1	32.8\pm0.9	33.1\pm1.0	34.0\pm1.0	35.1\pm1.8

normalization and dropout. For classifier h , we adopt one fully connected layer with softmax function. For group discriminator D , we adopt 3 connected layers with softmax function. For objects tasks, we employ Densenet-169 [12] as encoder g .

Network hyper-parameters. We set fixed hyper-parameters in every method which is irrelevant to dataset, based on the common protocol of domain adaptation [34]. The batch size of generator is set to 32, and the batch size of group discriminator, encoder, classifier is all 64. We pre-train the group discriminator for 100 epochs. Meanwhile, the numbers of training steps of generator, group discriminator, encoder, classifier are set to 500, 50, 50, 50, respectively. Adam optimizer is with the same learning rate of 1×10^{-3} in generators, encoder, classifier and group discriminator. The tradeoff parameter β in Eq. (9) is set to $\frac{2}{1+\exp(-10\hat{q})} - 1$, same as [26]. And the tradeoff parameter λ in Eq. (7) is set to 0.2 fixed. For the fair comparisons, we only resize and normalize the image and do not use any addition data augment or transformation. Note than, for each experiment, we report the result of the model trained in the last epoch.

F Additional Experiments about HTL

In this section, we compare TOHAN with another novel HTL method, i.e., *dynamic knowledge distillation for HTL* (dkdHTL) [49]. It is worth noting that dkdHTL is a black-box HTL method. That is, we cannot access the parameters of source model. Therefore, in distillation loss, we cannot get the logits, which is used to compute the soften probabilities with a high temperature $T > 1$. To address this problem, they tried to solve the logits through soften probabilities approximately. For the sake of fairness, we convert dkdHTL to white-box version. Specifically, we use the standard softmax function in distillation loss, instead of the approximate version. Moreover, we initial the parameters of target model by source model. Then, we show the results of dkdHTL in Table 4 and Table 5.

We find that TOHAN outperforms dkdHTL in most tasks significantly. However, in $S \rightarrow M$, $U \rightarrow M$, and $S \rightarrow U$, there exists few tasks that dkdHTL outperforms TOHAN. In these three tasks, the complexity of source domain is high, while the complexity of target domain is low. TOHAN cannot generate qualified intermediate data effectively when the number of target data is very few and the source domain is highly complex simultaneously. dkdHTL is only suitable for tasks with uncomplicated target domain. The main

reason is that the training data of dkdHTML are only the few target data. If the target domain is complex, it is very easy to overfit. Therefore, as for tasks with complex target domains, TOHAN has the upper hand.

Table 5: Comparison between dkdHTML and TOHAN. We report the classification accuracy \pm standard deviation (%) on 2 objects FHA tasks: CIFAR-10 \rightarrow STL-10 and STL-10 \rightarrow CIFAR-10. Bold value represents the highest accuracy (%) among TOHAN and benchmark solutions.

Tasks	dkdHTML	TOHAN
CIFAR-10 \rightarrow STL-10	70.8 \pm 0.7	72.8\pm0.1
STL-10 \rightarrow CIFAR-10	52.4 \pm 0.5	56.6\pm0.3

G Additional Analysis

Visualization of Results. We use t-SNE to visualize the feature (the penultimate layer of the classifier) extracted by TOHAN and 5 benchmark solutions on $M \rightarrow U$ task (see Figure 7). When we use WA and FT methods, nearly all classes mix together. Although the classification accuracy of SHOT, S+F and T+F are relatively high, there are still a little mixtures among classes. For TOHAN, all classes are separated well, which demonstrates that TOHAN works well for solving FHA problem.

Detailed Analysis of Ablation Study. Table 6 shows the full results of ablation study. It is clear that TOHAN performs better than the corresponding two-step approach ST+FADA. However, when the number of target data is too small, ST+FADA may outperform TOHAN with a small probability. The reason for this abnormal phenomenon may be the limitation of target data. Although we use the technique of paring data, overfitting still occurs when data are scarce.

Table 6: Ablation Study. Bold value represents the highest accuracy (%) on each column. Data behind '+' is the standard derivation.

Tasks	FHA Methods	Number of target data						
		1	2	3	4	5	6	7
$M \rightarrow S$	S+FADA	25.6±1.3	27.7±0.5	27.8±0.7	28.2±1.3	28.4±1.4	29.0±1.0	29.6±1.9
	T+FADA	25.3±1.0	26.3±0.8	28.9±1.0	29.1±1.3	29.2±1.3	31.9±0.4	32.4±1.8
	ST+FADA	25.7±0.7	28.1±0.9	28.5±1.2	29.2±1.0	29.2±0.8	31.3±1.7	32.0±0.8
	TOHAN	26.7±0.1	28.6±1.1	29.5±1.4	29.6±0.4	30.5±1.2	32.1±0.23	33.2±0.8
$S \rightarrow M$	S+FADA	74.4±1.5	83.1±0.7	83.3±1.1	85.9±0.5	86.0±1.2	87.6±2.6	89.1±1.0
	T+FADA	74.2±1.8	81.6±4.0	83.4±0.8	82.0±2.3	86.2±0.7	87.2±0.8	88.2±0.6
	ST+FADA	74.3±1.2	83.7±1.0	83.8±0.8	85.8±0.6	86.0±0.9	87.7±0.8	89.0±0.6
	TOHAN	76.0±1.9	83.3±0.3	84.2±0.4	86.5±1.1	87.1±1.3	88.0±0.5	89.7±0.5
$M \rightarrow U$	S+FADA	83.7±0.9	86.0±0.4	86.1±1.1	86.5±0.8	86.8±1.4	87.0±0.6	87.2±0.8
	T+FADA	84.2±0.1	84.2±0.3	85.2±0.9	85.2±0.6	86.0±1.5	86.8±1.5	87.2±0.5
	ST+FADA	86.1±1.5	87.1±1.6	86.9±0.7	87.9±1.1	88.0±1.2	88.3±0.7	88.5±1.3
	TOHAN	87.7±0.7	88.3±0.5	88.5±1.2	89.3±0.9	89.4±0.8	90.0±1.0	90.4±1.2
$U \rightarrow M$	S+FADA	83.2±0.2	83.9±0.3	84.9±1.2	85.6±0.5	85.7±0.6	86.2±0.6	87.2±1.1
	T+FADA	82.9±0.7	83.9±0.2	84.7±0.8	85.4±0.6	85.6±0.7	86.3±0.9	86.6±0.7
	ST+FADA	84.0±0.7	84.2±0.5	85.3±1.0	85.6±1.2	86.7±1.0	86.5±0.5	88.0±1.0
	TOHAN	84.0±0.5	85.2±0.3	85.6±0.7	86.5±0.5	87.3±0.6	88.2±0.7	89.2±0.5
$S \rightarrow U$	S+FADA	72.2±1.4	73.6±1.4	74.7±1.4	76.2±1.3	77.2±1.7	77.8±3.0	79.7±1.9
	T+FADA	71.7±0.6	74.3±1.9	74.5±0.8	75.9±2.1	77.7±1.5	76.8±1.8	79.7±1.9
	ST+FADA	73.1±0.9	75.2±1.3	75.9±0.8	76.3±1.5	78.3±1.6	79.1±1.7	79.7±1.6
	TOHAN	75.8±0.9	76.8±1.2	79.4±0.9	80.2±0.6	80.5±1.4	81.1±1.1	82.6±1.9
$U \rightarrow S$	S+FADA	28.1±1.2	28.7±1.3	29.0±1.2	30.1±1.1	30.3±1.3	30.7±1.0	30.9±1.5
	T+FADA	27.5±1.4	27.9±0.9	28.4±1.3	29.4±1.8	29.5±0.7	30.2±1.0	30.4±1.7
	ST+FADA	28.1±1.3	28.9±0.7	29.2±1.5	29.8±1.2	31.0±0.9	31.2±0.9	33.2±1.7
	TOHAN	29.9±1.2	30.5±1.2	31.4±1.1	32.8±0.9	33.1±1.0	34.0±1.0	35.1±1.8